Hybrid Curved Precast Deep Beams Composed Partially from Concrete Made with Recycled Concrete Aggregate

Qasim M. Shakir[1, a *] and Asmaa F. Alghazali[1, b]

[1]Department of Civil Engineering, University of Kufa, Najaf, Iraq

[a]qasimm.alabbasi@uokufa.edu.iq and [b]asmaaf.alghazali@uokufa.edu.iq

*Corresponding author

Abstract. The present work presents the results of the experimental investigation of using crushed concrete as recycled coarse aggregates (RCA) and new models of hybrid deep beams. Six specimens of deep beams have been tested under static loads: two specimens as controls and three hybrid specimens with different types of hybridization models for concrete sections (horizontal, curved, and arched). This study aims to search for the optimum distribution of the concrete types for the hybrid deep beams such that the lowest cost is obtained and the RCA obtained from building demolition waste is introduced into the concrete mixes at 100%. The behavior has been tracked by the cracking and failure loads, loading history, crack width, and toughness. It was found that the capacities increased by 7.7, 18.7, 17.2, and 28.2%, respectively, in the horizontal, curved, arched, and arched with inclined stirrups hybrid models compared to the control specimen with RCA. Moreover, toughness was enhanced for the same specimens by 50.9, 71.1, 100.5, and 144.6%, respectively, compared to the control specimen with RCA.

Keywords: Precast deep beam, hybrid arched, steel fiber concrete, sustainable, recycled aggregate.

1. INTRODUCTION

Reinforced concrete deep beams are beams with a shear span to an overall depth greater than 2.0 ACI 318-19 [1]. Due to their high resistance capacity, reinforced concrete deep beams are used to transfer loads in several practical applications, such as high-rise buildings, foundation beams, panel beams, shear walls, water tanks, transfer beams, and deep girders [2]. Deep beams are one of the categories of D-regions, which include several members such as dapped ends [3,4], corbels [5], beam-column joints, pile caps, opening regions, stepped beams [6-10], etc. High disturbance of the flow of stress contour lines occurred at such regions due to large shear forces or concentrated loading, a sudden change in geometry, or a sudden change in cross-sectional area. To improve the behavior of deep beams, steel fibers are used. Sagi [11] studied RC deep beam specimens made of hybrid fibers (0.25% macro hooked-ended steel fibers and 0.25% macro synthetic fibers). Results showed that the ultimate load increased by adding 0.5% of fibers. Nayak [12] tested deep beams with varying fiber volume fractions (0, 1.5, and 3%). Results showed that the deep beams with 1.5% and 3% fiber fractions had a higher load-carrying capacity and cracking stress. Do-Dai [13] concluded that using steel fibers improved the shear resistance of deep beams as well as shear crack width, deflection, and concrete diagonal-cracking tensile strain. Abbas [14] concluded that the addition of deep fibers improved ductility, crack pattern, shear strength, and load-displacement behavior.

Sustainable construction refers to using recycled waste materials in concrete as a partial or full replacement. Construction wastes may be used as recycled aggregate, including ceramics, crushed glass, concrete, chopped rubber tires, bricks, wood, plastic, etc. [15]. Many researchers have studied the use of construction waste. Rather than employing natural coarse aggregates, the majority of efforts were focused on recycling as recycled asphalt pavement (RAP) and recycled concrete aggregate (RCA) [16]. Sérifou [17] studied the use of fine and coarse aggregates recycled from concrete waste. Tabsh and Abdelfatah [18] studied the influence of recycled concrete aggregates on the strength properties of concrete. Limbachiya [19] studied the influence of using recycled concrete aggregate (RCA) in high-strength concrete. Rao [20] reported that 25% RCA has no effect on concrete strength. Beyond this, the effect may increase with an increase in the amount of RCA. Seara-Paz [21] ascertained that the high replacement percentage reduces the strength, cracking resistance, and tensile splitting strength compared to conventional concrete. Arabiyat [22] studied experimentally and theoretically the behavior of concrete beams with recycled aggregates. Results showed that increased RCA replacement ratio decreased compressive strength and shear capacity. Regarding deep beams, Alhussein [23] concluded that when the RCA replacement ratio increased to 25%, 50%, and 75%, The compressive strength, splitting tensile strength, and modulus of elasticity decreased to values of (4, 13, and 23%), (1, 13, and 21%), and (2, 6, and 12%), respectively.

In recent years, hybrid deep beams with different hybridization models have been developed to control costs without severe performance drops. Several proposals have been suggested and examined. In this regard, Ali and Zghair [24] tested hybrid deep beams of the two layers of concrete, normal-strength concrete (NSC) and high-strength concrete (HSC), in the tension and compression zones, respectively. Results showed that when using HSC (about 45 N/mm^2) with a layer of thicknesses of 25–50% of the total beam depth, the ultimate shear strength increased by approximately 11–20% for beams without web reinforcement and by 17–22% for beams with minimum web reinforcement. Hassan and Faroun [25] proposed a model with fibrous concrete placed on both sides of the beam in the shear span area and normal concrete in the middle part. It was found that the ultimate load rate in the case of repeated loads reduces by (27% and 25%) when the fiber

ratio is 1% and 2%, respectively, and decreases by (21 and 19%) in the case of conventional concrete and fibrous concrete, respectively. Shakir and Hanoon [26] proposed a new hybridization model called the curved model. Steel fiber concrete (SFC) was used above the interface, and lightweight concrete (LWC) was used below it. It was observed that the capacities improved by 23 and 27% for the conventional hybrid model for the two loading systems, respectively. Moreover, the conventional hybrid model enhanced toughness by 44.7% and 143.7%, respectively. The study was extended by Shakir and Hanoon [27], which included using the reactive powder concrete (RPC) within the top layer to investigate the range of improvement in behavior. It was observed that the capacity increased in the horizontal and arched hybrid models by 27.6 and 39%, respectively, with the one-point system, while for tests under two-point loads, capacity enhanced by 34 and 36.9%, respectively. This research provided an improved hybrid model of sustainable deep beams made of steel fiber and RCA concrete based on the strut and tie model (STM). Two hybridization models have been proposed, and the results are compared with the conventional hybrid model. The proposed models aim to produce deep beams that qualify the requirements of high performance, low cost, and sustainability by incorporating recycled aggregate within the concrete out of the stress transfer path.

2. METHODOLOGY

2.1 Specimens Description

The experimental program included testing six deep beams, each with a total depth of 450 mm, a width of 160 mm, a clear span of 1400mm, and a total span of 1600 mm. The test was conducted with a one-point load at mid-span. Two beams are considered reference specimens; specimen CTRL-R100 represents the lower limit of the expected results. At the same time, specimen CTRL-SFC represents the upper limit. The other four specimens are hybrid beams. Specimen HRL-R100, made with the conventional horizontal model, consists of SFC at the top and RCA at the bottom. Specimen CRV-R100 represents the proposed curved model. Whereas specimens ARC1-R100 and ARC2-R100 represent the proposed arched model with vertical and inclined stirrups, Figure 1 shows the three hybridization models. Moreover, the designations and definitions of the tested specimens are shown in Table 1.

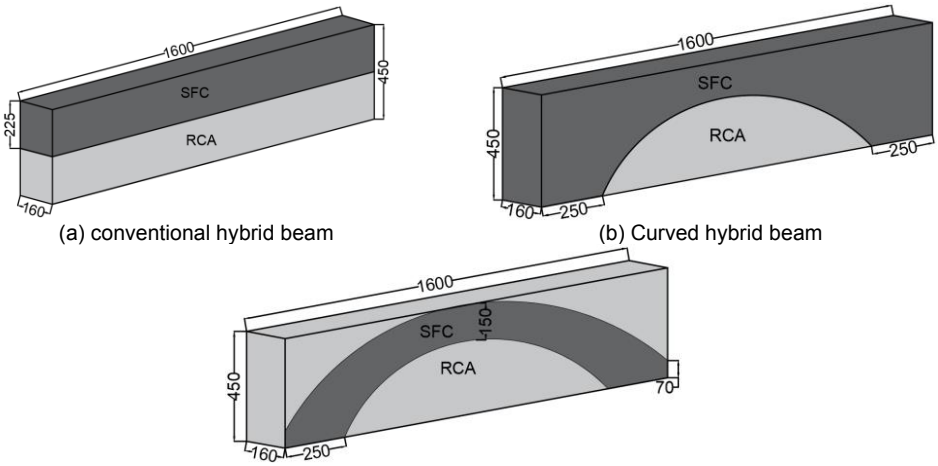

Figure 1**:** Details of the geometry of the deep beams (all units in mm).

Table 1: Designations of the tested specimens.

Coding	Detailing of hybridization
CTRL-R100	Control non hybrid with replacement 100%
CTRL-SFC	Control non hybrid steel fiber concrete
HRL-R100	Hybridization with replacement 100% within the lower half
CRV-R100	Curved hybridization with replacement 100% under the curved interface
ARC1-R100	Arched Hybridization vertical stirrups with replacement 100% out of the arch
ARC2-R100	Arched hybridization inclined stirrups with replacement 100% out of the arch

Bars of 8 mm diameter are used as stirrups and in strut reinforcement for the proposed models; bars of 10 mm are used as top reinforcement. While bars of (12 mm+16 mm) diameter are used as the main tensile (tie) reinforcement. Yield stress for bars of 8, 10, 12, and 16 mm (580, 560, 590, and 610) N/mm^2, respectively, and tensile strength (733, 713, 697, and 699) N/mm^2, respectively. The shear reinforcement, Ø8 @160, was calculated based on STM minimum reinforcement that should cross the strut elements [1]. Figure 2 shows details of the reinforcement specimen's deep beams.

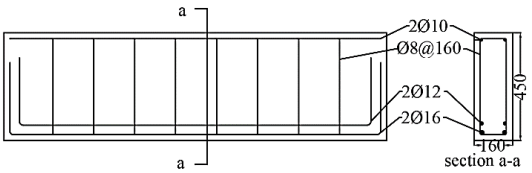

(a) Reinforcement for CTRL-SFC, CTRL-R100, and HRL-R100.

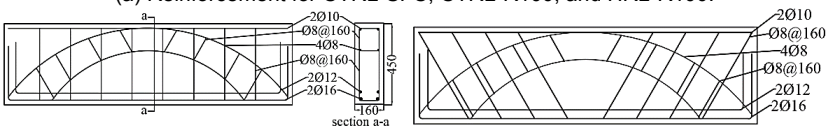

(b) Reinforcement for CRV-R100 and ARC1-R100. (c) Reinforcement for ARC2-R100.

Figure 2: Details of reinforcement of deep beam.

2.2 Materials

Ordinary Portland Cement (CAR) has been used and tested to qualify the requirements of Iraqi Specification No. 5, 1984 [28]. Natural sand was used as fine aggregate, and recycled concrete aggregates have been used in the normal concrete strength as a coarse aggregate mix with a maximum size of 20 mm. Natural crushed gravel has been used in the steel fiber concrete mix, with a maximum size of 14 mm. The physical properties tested were in accordance with Iraqi specification No. 45/1984 [29]. Table 2 shows the grain size analysis for fine and coarse aggregates. Limestone powder is used as a low-cost filler material to increase the amount of fines in the mix and enhance the workability of the concrete mix. Known locally as "Al-Gubra," it is a fine, white crushed powder. A superplasticizer, EPSILONE HP 580, has been used in concrete mixtures to reduce the water in the mix. It is used in both concrete mixes to test the results of the superplasticizer provided by the manufacturer, which qualifies the requirements of ASTM C-494 Type F and G [30]. Straight microsteel fibers with a diameter of 0.3 mm and a length of 13 mm have been used to enhance the shear resistance and improve the durability of the steel fiber concrete mix. Its testing complied with the standards of ASTM A 820-06 [31], and data from the manufacturer are provided.

Table 2: Grain size analysis of aggregate.

Sieve Size (mm)	Percent of Passing % of FA	Percent of Passing % of CA	%Passing limits Zone (2) [29]	
			FA Zone(2)	CA Zone(2)
20		99.10		95-100
14		86.45		80-90
10		36.10		30-60
5		2.30		0-10
4.75	98		90-100	
2.36	87		75-100	
1.18	74		55-90	
0.6	55		35-59	
0.3	22		8-30	
0.15	4.6		0-10	

2.3 Preparation of Recycled Coarse Aggregate

The RCA has been prepared as follows:

1) The wastes of concrete (cubes and cylinders after the test) are crushed to smaller sizes.
2) Sieving the natural gravel through sieves 20, 14, 10, and 5, and the remaining is sorted according to sieve size.
3) Sieving the crushed concrete through the same sieves 20, 14, 10, and 5, and the remaining particles are sorted according to the sieve size.
4) The RCA mix is provided by mixing the remaining quantities with the same values in the natural coarse aggregate. Figure 3 shows the recycled coarse aggregate and processing steps.
5)

(a) (b) (c) (d)

Figure 3: Details of recycled coarse aggregate: (a)The cubes and cylinders waste (b) Crushed concrete (c) Sieved the crushed concrete (d) mixes in proportions

2.4 Mechanical Properties of the Hardened Concrete

The test has been done for cylinders with dimensions of 100 mm in diameter and 200 mm in length to evaluate the splitting tensile strength (ft) according to ASTM C496-11 [32] and for cubes with dimensions of 100X100X100 mm to evaluate the cube compressive strength (fcu) according to BS 1881-116 1983 [33]. Cube compressive strength (fcu) N/mm^2. The results of the tests for steel fiber concrete SFC and normal strength concrete NSC were a compressive strength of 68 N/mm^2 and 42 N/mm^2, respectively, and a splitting tensile strength of 6 N/mm^2 and 2.3 N/mm^2, respectively.

2.5 Instrumentation and Testing Machine

The 2000 kN universal testing machine shown in Figure 4(a) was used for testing the reinforced concrete deep beams. The dial gauge is used to measure the deflection of the deep beam at two points. The crack width was measured by using a 0.5 mm-range crack meter. When the width of the fracture exceeded 0.5 mm, it was measured with a digital Verna. Figure 4(b,c,d) shows tools used in measuring response.

(a) (b) (c) (d)

Figure 4: (a) Loading machine, (b) dial gauge, (c) Vernia, (d) Crack meter.

2.6 Casting the Precast Hybrid Beams

The steel reinforcement was installed after preparing the forms such that the top side was (depth X length). Then, the dividing steel plates with slots cut out to pass the stirrup reinforcement were fixed. Following that, two mixers were used to mix the concrete, one for each type. Then, concrete was poured forms on both sides of the plate simultaneously. The dividing plates were taken off as soon as the specimen's casing was complete. No interface problem will consequently arise. In precast concrete factories, such casting procedures are simple to complete.

3. RESULTS AND DISCUSSION

3.1 Crack Patterns at Failure

3.1.1 Control Specimens (Specimens CTRL-SFC and CTRL-R100)

This specimen CTRL-SFC is tested to evaluate the effect of high-strength steel fiber concrete on the general behavior of a deep beam. The map of cracking for the control non-hybrid deep beam is shown in Figure 5(a), which reveals that the first crack appeared near the center at a load of 90 kN as a flexural crack and continued to extend vertically up to the point of load application. The first diagonal crack initiated at a level of 120 kN, following a path toward the point loads at the top of the beam. Additionally, cracks developed towards the compression face, resulting in a steady weakening of the compression face up to the level of 505 kN when the failure occurred as a flexural failure type. No crushing at the compression face and support regions has been observed. The ductile behavior may result from the use of steel fibers in concrete, and the STM used in designing the control beam yielded conservative results.

Moreover, it can be seen that no cracking occurred at the top corner regions and that the resistance may not have affected the development of the flexural cracking. Specimen CTRL-R100 is considered a control beam for samples containing normal-strength concrete with 100% replacement recycled coarse aggregate. The crack pattern for CTRL-R100 is shown in Figure 5(b) when the flexural cracks started to appear from the bottom at the middle of the beam at a load of 50 kN, recording a reduction in cracking load by 44.4% relative to CTRL-SFC. With progress in loading, more cracks developed on both sides of the flexural. At a level of 330 kN loading, the outermost diagonal crack that is expected to connect the point load with the support reaction was observed. However, some crushing at the compression face occurred. The beam failed at a load of 418 kN following a diagonal (flexural-shear) mode failure. Again, it can be observed that the corners did not contribute effectively to resistance (no cracking). Thus, it is expected that using low-strength concrete in these regions may not affect the response significantly.

3.1.2 Conventional Hybrid Beam (Specimen HRL-R100)

This specimen represents the well-known conventional hybrid deep beams that are aimed to increase the compressive strength of the top part at which the top nodal point lies (CCC node). Steel-fiber concrete was used in the top layer of HRL-R100, while normal-strength concrete with 100% replacement was used in the bottom layer. The failure of the control specimen CTRL-R100 is expected to be due to the exhaustion of the

compression resistance induced by the compression block due to the development of flexural cracks with the progress of loading. Figure 5(c) shows the map of the crack propagation at the failure, where the first crack began as a flexural crack in the mid-span at loading 50 kN. The crack developed vertically with progressive loading, and other cracks spread horizontally on both sides with decreased angles away from the flexural crack. Shear cracks developed diagonally upward towards the loading point. The steel fiber at the top of the concrete slows crack propagation when it reaches the layer of steel fiber concrete. However, most cracks are prevented from forming within the top layer, preventing the formation of actual (full) diagonal cracks around or along the compression struts or cracks similar to the semi-diagonal diagonal cracks in the corresponding control specimen. The failure occurred at 450 kN of load as a flexural-shear mode failure. Compared to the reference specimens CTRL-R100 and CTRL-SFC, the capacity of the hybrid deep beam increased by 7.7% compared with CTRL-R100 and decreased by 10.9% compared with CTRL-SFC. The same behavior at the top corners can be seen.

3.1.3 First Proposed Hybrid Model (Specimen CRV-R100)

In this model, steel fiber concrete (SFC) was used in the region above the curved interface, as shown in Figure 2(b), to improve the efficiency of stress transfer at contact points with supports, which was designed in a strut and tie model, and RCA with 100% replacement was added in the tie region. Figure 5(d) shows the crack propagation history for the hybrid deep beam CRV-R100. It can be noted that the first crack initiated at the mid-span at 40 kN. Nonetheless, the arching action and the high-strength concrete SFC limited the excessive curvature and later fracture development. The model failed with flexural-shear failure mode when the load reached 496 kN. The use of the curved distribution of concrete and steel reinforcement in the struts region led to an improvement in the capacity of the deep beam to 18.7% and 10.2% compared to the control model CTRL-R100 and the conventional hybrid model HRL-R100, respectively, despite the use of normal concrete with 100% replacement in the tension area. The capacity of the beam decreased by 1.7% compared to the control model CTRL-SFC.

3.1.4 Second Proposed Hybrid Model (Specimens ARC1-R100 and ARC2-R100)

In this model, ARC1-R100, steel fiber concrete was used only in the compression strut region, with additional reinforcement of 8 @ 160 mm C.C., and RCA with 100% replacement was used above and below the arch compressive zone of the deep beam. The history of the crack pattern for specimen ARC1-R100 is shown in Figure 5(e). At a load of 40 kN, the first flexural crack appeared at the mid-span of the beam, and it started spreading within the RCA (nonfibrous), gradually ascending to the steel fiber concrete. This specimen failed due to flexural mode failure in the mid-span at 490 kN, with the capacity of this model increasing by 17.2% and 8.89% when compared to CTRL-R100 and HRL-R100, respectively. Compared to CTRL-SFC and CRV-R100, the beam's capacity decreased by 2.97% and 1.2%, respectively. For ARC2-R100, it can be seen from the previous discussions that the diagonal cracking is affected partially by concrete strength developed generally along the compression struts. Figure 5(f) shows the crack pattern's history. Thus, it is aimed to restrict the development of such cracking by changing the angle of stirrups to be normal to the compression struts. The same arrangement of specimen, ARC1-R100 was used, with the expectation regarding the orientation of the stirrups. It can be observed that the first crack appeared in the mid-span at 50 kN of loading. Additional cracks developed on both sides of the mid-span and propagated toward the top compression zone, while diagonal cracks formed at 160 kN. The failure occurred at a load of 536 kN with a flexural mode failure. The capacity of the deep beam was enhanced as it increased by 28.23% and 6.13% compared to the control specimens CTRL-R100 and CTRL-SFC, respectively. It's enhanced by 19.1%, 8%, and 9.4% compared to HRL-R100, CRV-R100, and ARC1-R100, respectively.

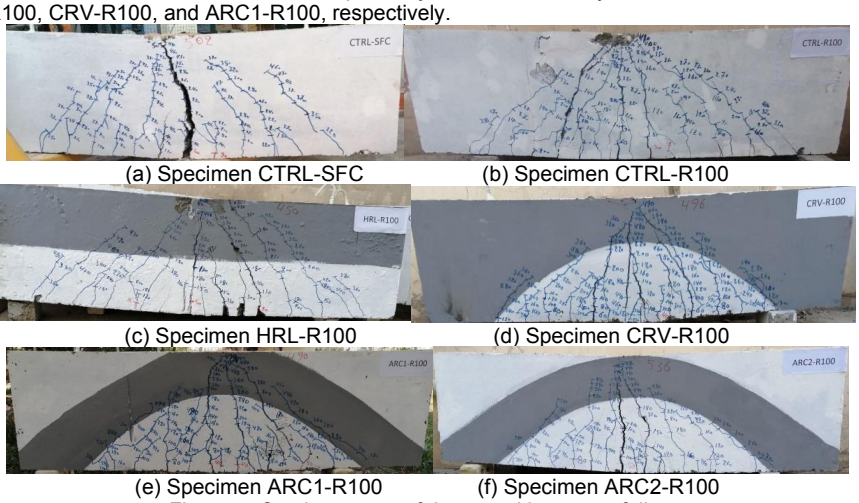

(a) Specimen CTRL-SFC (b) Specimen CTRL-R100

(c) Specimen HRL-R100 (d) Specimen CRV-R100

(e) Specimen ARC1-R100 (f) Specimen ARC2-R100

Figure 5: Crack patterns of the tested beams at failure.

3.2 Load-Deflection Curves

Figure 6 shows the load-deflection curve of deep beam specimens. It can be seen that the load-deflection curve for all specimens consists of two linear segments. The linear part ended in the range of 390 kN, i.e., 73% of the failure load. It can be seen that the specimen CTRL-R100 recorded the lowest value, while the specimen CTRL-SFC yielded the largest stiffness. Moreover, it is clear that the specimen CRV-R100 yielded stiffness very close to that of the specimen CTRL-SFC, whereas the specimen ARC2-R100 yielded a slightly smaller stiffness. It can be concluded that the proposed hybrid models improved the initial stiffness relative to the conventional hybrid model. Furthermore, it can be observed that there is a sudden change in stiffness for specimen CTRL-R100, whereas a gradual change can be noticed for other beams. This demonstrates that the cracking and stress transfer rate from concrete to steel was generally uniform. For the second part of the load-deflection curve, it can be observed that the stiffness of specimen CTRL-R100 was very close to zero (horizontal), and it increased gradually from the conventional hybrid beam, recording the highest value for specimen ARC2-R100. This means that the beam's strength is fully exhausted for specimen CTRL-R100. Consequently, a mechanism should be provided when it is intended to strengthen such beams. The results of specimen ARC2-R100 reveal that higher capacities may be obtained if more tension steel (tie reinforcement) is used. The ultimate load and maximum deflection are shown in Table 3.

For specimen HRL-R100, it can be noted that some softening occurred at the early stage, as in the control specimen CTRL-R100. After that, the stiffness increased to a higher level; it was 50.6 kN/mm, which was kept constant up to 360 kN. For the specimen, CRV-R100, the changes in stiffness started at an earlier stage. Initial stiffness was 61.8 kN/mm, which remained constant up to 400 kN loading; after that, the stiffness decreased gradually. In specimen ARC1-R100, the stiffness remains constant with an initial stiffness of 53.6 kN/mm up to a load of 370 kN. Then, the stiffness begins to decrease. The initial stiffness of specimen ARC2-R100 was 55.2 kN/mm, which was kept continuously up to 400 kN. Beyond that, the stiffness gradually decreased due to crack propagation through the bottom normal concrete layer.

3.3 Toughness

Toughness measures a member's ability to absorb deformations before failure. It is also the area under the load-deflection curve, which the dissipated energy is generated by member deterioration up to failure [34-36]. Figure 7 shows the toughness variation for the tested deep beam specimens. The control specimen CTRL-R100 has the lowest toughness, which is 3210 kN.mm, while CTRL-SFC has a toughness of 7691 kN.mm. When using the SFC layer for the hybrid HRL-R100, CRV-R100, ARC1-R100, and ARC2-R100, the toughness improved by 50.9%, 71.1%, 100.5%, and 144.6%, respectively, compared with the control specimens CTRL-R100, because the SFC covers most of the strut area and included all D-region of the deep beam. It can be observed that the proposed models yield higher values of toughness. Due to the arching action within the hybrid beams that restricts failure and provides an efficient path for load transfer to the supports.

Table 3: Experimental test results of specimens.

Specimens	Cracking load p_{cr} (kN)	Ultimate load pu (kN)	Max. deflection (mm)	Max. width of flexural crack (mm)	Max. width of diagonal crack (mm)
CTRL-SFC	90	505	20.25	6	0.3
CTRL-R100	50	418	12.26	3.94	0.41
HRL-R100	50	450	13	3.89	2
CRV-R100	40	496	16	3.02	0.6
ARC1-R100	40	490	18.82	3.9	0.43
ARC2-R100	50	536	21	5.9	0.4

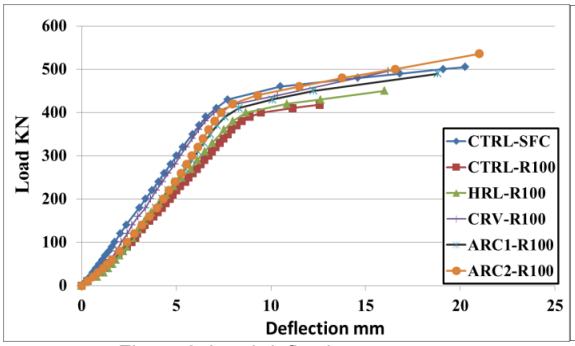

Figure 6: Load-deflection curves.

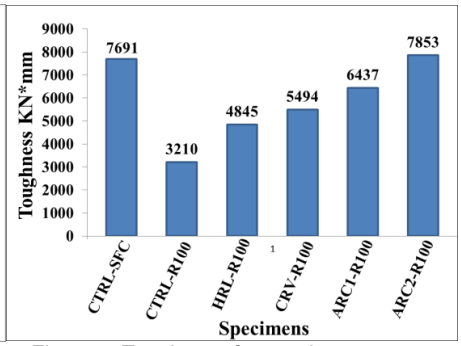

Figure 7: Toughness for specimens.

3.4 Crack Width

Figure 8(a) shows the rate of widening of the flexural cracking for the tested specimens.370 kN. It can be observed that for specimen CTRL-R100, the rate is slow up to a load of 370 kN. Beyond this, the crack widened rapidly, recording a crack width of 3.94 at failure. For specimen HRL-R100, gradual widening was observed

up to the load level of 400 kN. After that, a higher rate of crack development was noticed, recording a maximum crack width of 3.89 mm. For specimen CRV-R100, it can be seen that the load at which the cracks widened rapidly was 460 kN. Beyondthis,, cracking developed at a smaller rate relative to the CTRL-R100, referring to thearching effect For the second proposal, specimen ARC1-R100, the flexural crack widened slowly up to a load of 400 kN. Then, the widening rate increased at a higher rate, recording a maximum value of 3.9 mm. The effect of strengthening the beam ARC2-R100 against diagonal cracking by making the stirrups normal to the crack was that the rate of flexural cracking was significantly reduced. Load level of 400 kN, and the crack widened at a higher rate up to the failure. Figure 8(b) shows the rate of widening of diagonal cracking. It can be observed that in all specimens, the maximum width is less than the flexural. This refers to the ductile behavior of the tested specimens. Specimen CTRL-SFC recorded the lowest rate because of the effect of fiber addition, while a higher rate can be seen for specimen CTRL-R100, with some fluctuation in the range of 300–400 kN due to the transfer of stresses. For specimen HRL-R100, the width of the diagonal crack increased slightly up to a load of 400 kN. After that, the maximum cracking recorded was 2 mm. For specimens CRV-R100, ARC1-R100, and ARC2-R100, the maximum cracking recorded was 0.6 mm, 0.43 mm, and 0.4 mm, respectively.

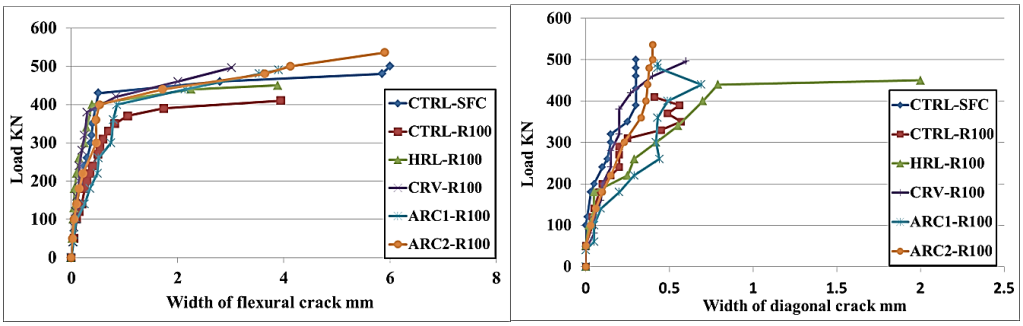

(a) Rate of widening of the flexural cracks. (b) Rate of widening of the diagonal crack.

Figure 8: Crack width of specimens.

4. CONCLUSIONS

Based on the test of the deep beam specimens, the following conclusions can be drawn:

- It found that the capacities increased by 7.7, 18.7, 17.2, and 28.2% in the horizontal, curved, arched, and arched with inclined stirrups hybrid models compared to the control specimen CTRL-R100. Also, the capacity increased by 6.1% for the arched with inclined stirrups hybrid model compared to the control specimen CTRL-SFC but decreased by 10.9, 1.8, and 2.9%, respectively, in the horizontal, curved, and arched hybrid models.
- The result revealed that the top corner of all specimens has a minor effect on resistance and the central region, where the crack is vertical, so that the RCA may be used within such regions without a severe drop in performance.
- When using the hybridization systems, the horizontal, curved, arched, and arched with inclined stirrups hybrid models' toughness increased by 50.9, 71.1, 100.5, and 144.7%, respectively, compared to the control specimen CTRL-R100. The steel reinforcement design for the deep beams that cross the compression strut, as recommended by the STM models, may produce some ductile behavior, and the beams may fail by flexural cracking, according to test results.
- Regarding crack width, the proposed arched model ARC2-R100 showed almost similar results to CTRL-SFC for the width of flexural and diagonal cracks.

REFERENCES

[1] ACI Committee 318-19. Building code requirements for structural concrete. Farmington Hills, Michigan: American Concrete Institute. 2019.

[2] Yang, K. H., and Ashour, A. F. Load capacity of reinforced concrete continuous deep beams. Journal of structural engineering. 2008; 134(6): 919-929.

[3] Campione G, LaMendola L, Papia M. Steel fiber reinforced concrete corbels: experimental behavior and shear strength prediction. ACI Struct J. 2007; 104(5):570–597.

[4] Shakir Q. M., Abd Alsaheb S.D., Farsangi E. N. Rehabilitation of deteriorated reinforced self‐consolidating concrete brackets and corbels using CFRP composites: diagnosis and treatment. Journal of Building Pathology and Rehabilitation. 2023.

[5] Shakir Q. M. and Abd Alsaheb S. D. High strength self-compacting corbels retrofitted by near surface mounted steel bars. Pollack Periodica. 2022.

[6] Shakir Q. M., Al-Sahlawi Y. M., B.B. Abd and Hamad S. A. Nonlinear Finite Element Analysis of High-strength Reinforced Concrete Beams with Severely Disturbed Regions. Jordan Journal of Civil Engineering. 2023; 17(10).

[7] Fayed S., Basha A., Elsamak G. Behavior of RC stepped beams with different configurations: An experimental and numerical study. Structural concrete. 2020.
[8] Shakir Q. M., Hamad S. A. Enhancement of the Behaviour of Reinforced Concrete Dapped End Beams Including Single pocket Loaded by a Vertical Concentrated Force. Engineering Review. 2023.
[9] Shakir Q.M., Hamad SA. Behavior of pocket-type high strength RC beams without or with dapped ends. Pract. Period. Struct. Des. Constr. 2021; 26(4): 04021048.
[10] Mogili S. and Hwang S.-J. Softened Strut-and-Tie Model for Shear and Flexural Strengths of Reinforced Concrete Pile Caps. Journal of Structural Engineering, ASCE. 2021; 147(11).
[11] Sagi M. S. V, Lakavath C, Prakash S. S, and Sharma A. Experimental study on evaluation of replacing minimum web reinforcement with discrete fibers in RC deep beams. Fibers. 2021; 9(11): doi: 10.3390/fib9110073.
[12] Nayak C. B. Experimental and numerical study on reinforced concrete deep beam in shear with crimped steel fiber. Innov. Infrastruct. Solut. 2022; 7(1). doi: 10.1007/s41062-021-00638-2.
[13] Do-Dai, T., Tran, D. T., and Nguyen-Minh, L. Effect of fiber amount and stirrup ratio on shear resistance of steel fiber reinforced concrete deep beams. Journal of Science and Technology in Civil Engineering (STCE)-HUCE. 2021; 15(2): 1-13.
[14] Abbas, Y. M., Tuken, A., and Siddiqui, N. A. Improving the structural behavior of shear-deficient RC deep beams using steel fibers: Experimental, numerical and probabilistic approach. Journal of Building Engineering. 2022; 46(1): 103711.
[15] Ju, H., Yerzhanov, M., Serik, A., Lee, D., and Kim, J. R. Statistical and reliability study on shear strength of recycled coarse aggregate reinforced concrete beams. Materials. 2021; 14(12): 3321.
[16] Soltanabadi, R., and Behfarnia, K. Shear strength of reinforced concrete deep beams containing recycled concrete aggregate and recycled asphalt pavement. Construction and Building Materials. 2022; 314(1): 125597.
[17] Sérifou, M., Sbartai, Z. M., Yotte, S., Boffoué, M. O., Emeruwa, E., and Bos, F. A study of concrete made with fine and coarse aggregates recycled from fresh concrete waste. Journal of Construction Engineering. 2013.
[18] Tabsh S. W. and Abdelfatah A. S. Influence of recycled concrete aggregates on strength properties of concrete. Constr. Build. Mater. 2009; 23(2).
[19] Limbachiya M, Meddah M. S, and Y. Ouchagour Y. Use of recycled concrete aggregate in fly-ash concrete. Constr. Build. Mater. 2012; 27(1).
[20] Rao M. C, Bhattacharyya S. K, and Barai S. V. Behaviour of recycled aggregate concrete under drop weight impact load. Constr. Build. Mater. 2011; 25(1).
[21] Seara-paz S, González-fonteboa B, Martínez-abella F, and Eiras-lópez J. Flexural performance of reinforced concrete beams made with recycled concrete coarse aggregate. Eng. Struct. 2016; 156(1).
[22] Arabiyat S, Jaber A, Katkhuda H, and Shatarat N. Influence of using two types of recycled aggregates on shear behavior of concrete beams. Constr. Build. Mater. 2021; 279(1): 122475.
[23] Hussein Amer Alhussein, T., and Abdul Samad Khudhair, J. Experimental and numerical evaluation of shear strength of directly and indirectly loaded flanged recycled self-compacted reinforced concrete deep beams. Journal of Engineering. 2020.
[24] Yaser Ali, A., and Ghazi Zghair, M. Experimental investigation and nonlinear analysis of hybrid reinforced Concrete Deep Beams. Al-Qadisiyah, Journal for Engineering Sciences. 2015; 8(2): 99-119.
[25] Hassan, S. A., and Faroun, G. A. Behavior of hybrid reinforced concrete deep beams under repeated loading. Civil and Environmental Research. 2016; 8(10): 14-37.
[26] Shakir Q. M. and Hanoon H. K. Behavior of High-Performance Reinforced Arched- Hybrid Self-Compacting Concrete Deep Beams. Journal of Engineering Science and Technology. 2023; 18(1): 792–813.
[27] Shakir Q. M. and Hannon H. K. A Novel Hybrid Model of Reinforced Concrete Deep Beams with Curved Hybridization. Jurnal Teknologi. 2023; 2(1): 31–39.
[28] Iraqi Specification No. 5. Portland cement. Iraq, Baghdad.1984.
[29] Iraqi Specification No.45. Natural sources for gravel that is used in concrete and construction. Iraq, Baghdad. 1984.
[30] ASTM C494/C494M-13. Standard specification for chemical admixtures for concrete. Annual Book of ASTM Standard. 2013.
[31] ASTM A 820-06. Standard specification for steel fibers for fiber reinforced concrete. 2006.
[32] ASTM C496/C496M-11. Standard test method for splitting tensile strength of cylindrical concrete specimens. Annual Book of ASTM Standard. 2011.
[33] BS 1881-116. Method for determination of compressive strength of concrete cubes. British Standards Institute, London. 1983.
[34] Low N. M. P. And Beaudoin J. J. The flexural toughness and ductility of portland cement-based binders reinforced with wollastonite micro-fibres. Cem. Concr. Res. 1994; 24(2). doi: 10.1016/0008-8846(94)90050-7.
[35] Noushini A, Samali B, and Vessalas K. Flexural toughness and ductility characteristics of polyvinyl-alcohol fibre reinforced concrete (PVA-FRC). Proc. 8th Int. Conf. Fract. Mech. Concr. Concr. Struct. Fram. 2013.
[36] Shakir Q.M., and Abd B.B. Retrofitting of self-compacting RC half joints with internal deficiencies by CFRP fabrics. Jurnal Teknologi. 2020; 82(6): 49-62.